

University of Groningen

Surface sensitivity effects with local probe scanning Auger–scanning electron microscopy

Agterveld, D.T.L. van; Palasantzas, G.; Hosson, J.Th.M. De

Published in:
 Applied Physics Letters

DOI:
[10.1063/1.124603](https://doi.org/10.1063/1.124603)

IMPORTANT NOTE: You are advised to consult the publisher's version (publisher's PDF) if you wish to cite from it. Please check the document version below.

Document Version
 Publisher's PDF, also known as Version of record

Publication date:
 1999

[Link to publication in University of Groningen/UMCG research database](#)

Citation for published version (APA):

Agterveld, D. T. L. V., Palasantzas, G., & Hosson, J. T. M. D. (1999). Surface sensitivity effects with local probe scanning Auger–scanning electron microscopy. *Applied Physics Letters*, 75(8), 1080-1082. <https://doi.org/10.1063/1.124603>

Copyright

Other than for strictly personal use, it is not permitted to download or to forward/distribute the text or part of it without the consent of the author(s) and/or copyright holder(s), unless the work is under an open content license (like Creative Commons).

Take-down policy

If you believe that this document breaches copyright please contact us providing details, and we will remove access to the work immediately and investigate your claim.

Downloaded from the University of Groningen/UMCG research database (Pure): <http://www.rug.nl/research/portal>. For technical reasons the number of authors shown on this cover page is limited to 10 maximum.

Surface sensitivity effects with local probe scanning Auger–scanning electron microscopy

D. T. L. van Agterveld, G. Palasantzas, and J. Th. M. De Hosson^{a)}

Department of Applied Physics, Materials Science Center and Netherlands Institute for Metals Research, University of Groningen, Nijenborgh 4, 9747 AG Groningen, The Netherlands

(Received 1 March 1999; accepted for publication 30 June 1999)

This letter concentrates on a quantitative description of surface roughness effects on Auger peak-line profiles for pure and alloyed specimens. The nanometer lateral electron probe size of the order of 10 nm yielded peak-line profiles that capture surface topology variations down to nanometer-length scales. Surface roughness leads to peak-intensity fluctuations, which are described within the weak roughness limit by a simple form, $I(r) \approx I_{av}[1 + \beta h(r)]$. I_{av} is the average peak intensity, $h(r)$ represents the roughness fluctuation along a lateral in-planar distance r , and β is a constant (< 1). In addition, analyses of the peak-difference correlation function $I_z(r) = \langle [I(r) - I(0)]^2 \rangle^{1/2}$ showed a power-law behavior $I_z(r) \propto r^\alpha$ with α ranging between 0.7 and 1 at small-length scales, i.e., for $r \ll \xi$, with ξ a peak correlation length that was comparable to average specimen cluster sizes. © 1999 American Institute of Physics. [S0003-6951(99)04534-9]

With the advent of Auger electron spectroscopy (AES) in the 1960s, a wide range of surface analysis possibilities became feasible for fundamental and applied research.¹ AES yields chemical composition information for surface layers within the range of depth between about 0.3 and 5 nm, depending on the peak energy. Application of AES in applied fields of research, like microelectronics, catalysis, polymer, and metals technology has made it an extremely powerful tool, e.g., for understanding “impurity”-induced failure mechanisms and surface degradation mechanisms. Nonetheless, Auger peak intensities can be strongly affected by surface topology effects such as roughness.

So far, experimental studies have shown that the surface topology actually may have a substantial influence in depth resolution during depth profiling. It was shown that the roughness contribution Δh increases with sputtering depth z , following the relation (for normal ion incidence) $\Delta h \sim z$.² However, because up to now finite beam sizes of the order ~ 0.1 – $1 \mu\text{m}$ (or larger) were commonly used in AES, precise quantifications of topology effects were rather limited. Therefore, only scant research is available in the literature that focuses on the effects of surface roughness on peak-line profiles at a nanometer-length scale. Only recently has the introduction of field-emission electron guns in AES with nanometer beam spot sizes (~ 10 – 20 nm) (Ref. 3) opened the possibility for nanometer-scale quantification of roughness effects. This letter outlines a possible methodology and summarizes some results obtained.

To illustrate the basic principles, AES studies were performed on surfaces showing lateral roughness wavelengths ranging from $\sim 50 \text{ nm}$ to a few microns in lateral size (Fig. 1). We calculated peak-difference correlation functions on various samples and estimated their characteristics at length scales that are sufficient to capture the essence of roughness fluctuations in a manner similar to other techniques [e.g., x-ray reflectivity, scanning tunneling and atomic force mi-

croscopy (STM, AFM), etc.].⁴ The AES measurements were performed in a specially designed local probe scanning Auger–scanning electron microscope (SAM/SEM), equipped with a field-emission gun (derived from a JEOL-JAMP 7800F), with a base pressure $\sim 2 \times 10^{-8} \text{ Pa}$. The operation conditions (emission current $2.4 \times 10^{-9} \text{ A}$ and accelerating voltage 10 kV) yielded a beam spot size of $\sim 15 \text{ nm}$. Surface cleaning (oxide removal) of all samples was performed by *in situ* Ar-ion sputtering (3 keV Ar⁺). No subsequent annealing took place. In all stages of preparation and measurement the samples were tilted to 30° with respect to the normal of the incident electron beam. Experimental observations are presented for pure Al [Fig. 1(a)] and an Al–Mg alloy [Fig. 1(b)]. In the latter case, the sample surface consisted of a rather random distribution of islands termed as “dark” (Al phase; low-Mg content $\sim 15 \text{ at. \% Mg}$), which are surrounded by *bright* areas (β phase; high-Mg content $\sim 38 \text{ at. \% Mg}$).

In the limit of weak roughness, the peak-difference correlation function $I_z(r) = \langle [I_a(r) - I_a(0)]^2 \rangle^{1/2}$ can be related directly to the surface height-difference correlation function $z(r) = \langle [h(r) - h(0)]^2 \rangle^{1/2}$ [Appendix, Eq. (A3)] via the relation $I_z(r) \approx (I_a^0 r_a X_a / \lambda_a^0 \cos \phi) z(r)$ with I_a^0 the intensity of an elemental bulk standard, r_a the backscattering factor, ϕ the angle of emission of the detected electrons with respect to the normal to the sample surface, and λ_a^0 the inelastic mean-free path or attenuation length of the electrons for a given energy.¹ Furthermore, from a wide variety of roughness studies,⁴ $z(r)$ is known to follow, in many cases, the scaling behavior $z(r) \approx \beta r^\alpha$ for $r \ll \xi$, and $(z(r))^2 \approx 2w^2$ for $r \gg \xi$ with α the so-called roughness exponent, ξ a lateral correlation length, and w the rms roughness amplitude.⁴ Direct one-dimensional height profiles were used in the past in roughness studies by STM,⁵ while in our case a similar analysis will be performed on Auger peak-line profiles.

To illustrate our point, Fig. 1(b) displays the variation of the peak intensity for Al (*KLL* peak, 1390 eV) in the Al–Mg alloy with the electron beam scanning along the indicated line, from a *bright* to a *dark* area. The peak intensity shows

^{a)}Corresponding author. Electronic mail: hossonj@phys.rug.nl

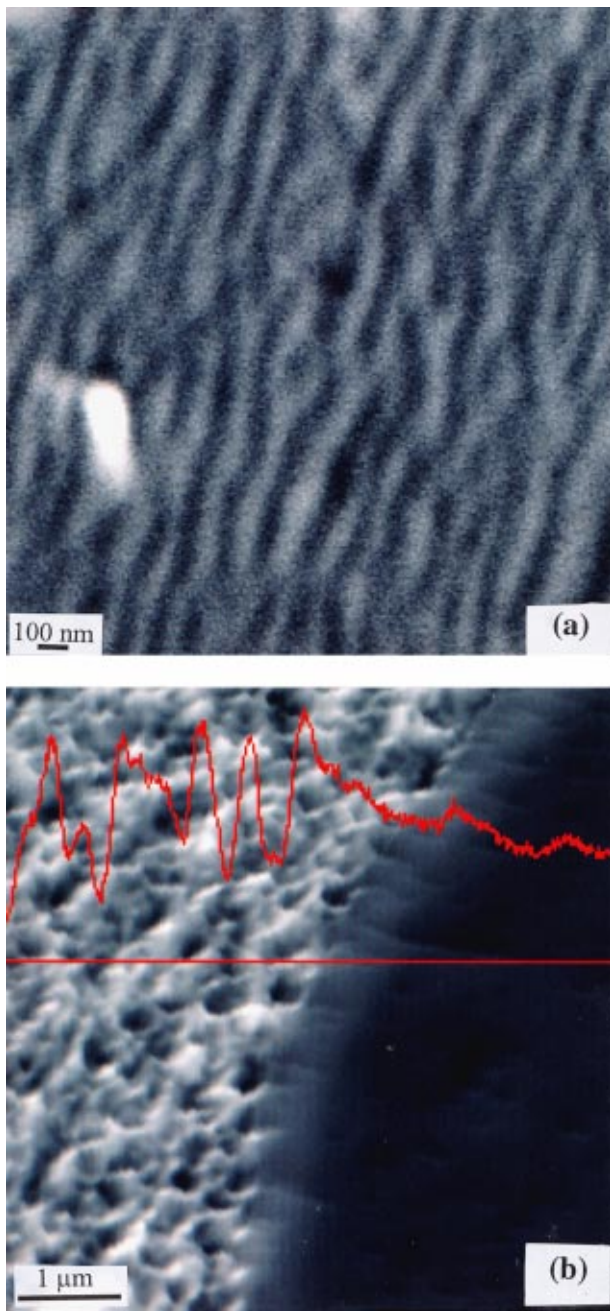


FIG. 1. SEM images of the various samples considered in the present study: (a) pure Al and (b) Al–Mg alloy, where an Al peak-line profile is shown, taken on the indicated line on the sample.

strong variations, closely following the variations of the local sample morphology. On the *bright* areas, the observed lateral roughness wavelengths are in the range ~ 500 nm, and thus, are sufficiently large not to be obscured by finite beam spot size effects. The surface morphology causes variations on the peak intensities, of the order of $\sim 25\%$ of the average signal (for Al). The intensity was higher on the bumps and lower on the valleys with an effective peak width that approximately corresponds to the size of the bump or valley. For the pure Al sample, [Fig. 1(a)], the variation in peak intensity was $\sim 4\%$ with respect to the average peak intensity.

The peak-line profile variation appears to have a quasi-periodic structure at length scales comparable to the average bump/valley size. Therefore, we assumed for simplicity a periodic roughness profile $h(r) = A \sin(2\pi r/\Lambda)$, with A the

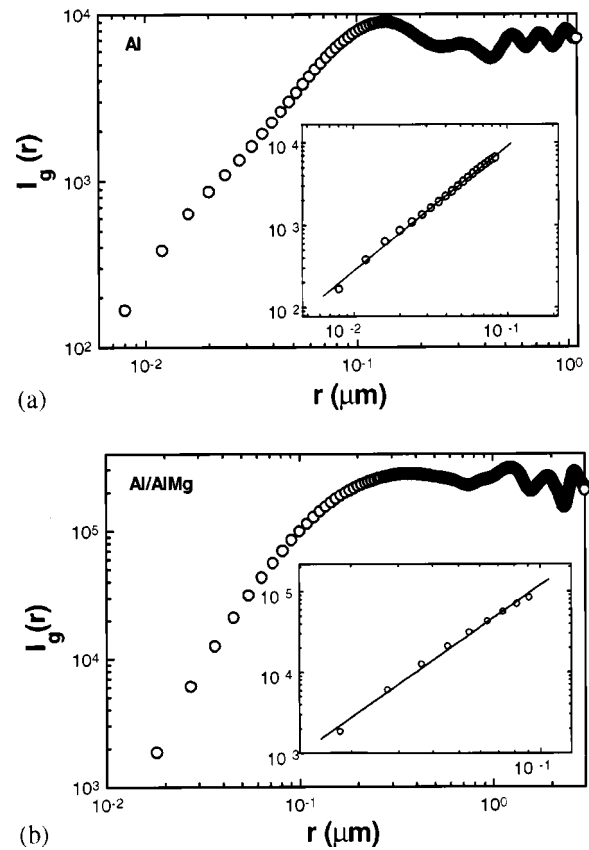


FIG. 2. Calculation of the variances of the peak-difference correlation function for: (a) pure Al and (b) Al in an Al–Mg alloy. The insets show the line fits to obtain the corresponding scaling exponents.

roughness amplitude and Λ the corresponding oscillation wavelength, as a first approximation to understand the roughness-induced fluctuations. For the specimens under consideration, the oscillatory behavior of the peak profiles (mainly, the minimum and maximum variation from the average line) can be reproduced by an expression, similar to that of the weak roughness limit expansion (see the appendix), of the form $I(r) = I_{av} [1 + Dh(r)/\lambda_a^0 \cos \phi^*]$ with $\cos \phi^* = [\sin \varphi (\partial h/\partial r) + \cos \varphi] / \sqrt{1 + (\partial h/\partial r)^2}$, I_{av} the average intensity and D a constant ($\approx 10^{-2}$). The corresponding roughness parameters A and Λ that yielded similar variations to that of the maximum–minimum peak variation were, respectively, pure Al: $A \approx 12$ nm and $\Lambda \approx 200$ nm; and the Al–Mg alloy: $A \approx 60$ nm and $\Lambda \approx 600$ nm. The corresponding average bump/valley size $L \approx \Lambda/2$ is well comparable to the sizes obtained from the SEM images, and the ratio $A/L \sim 0.1$ is consistent with the weak roughness limit expansion.

The variances I_g , i.e., the peak-difference correlation functions squared for the various peak-line profiles, are shown in Fig. 2. The pure Al surface exhibits a ripple-like structure (being produced by ion etching during sputtering⁴) with an average ripple size of ~ 100 nm, which is much larger than the beam spot size (by nearly an order of magnitude). The peak-line profiles were acquired along the x axis over a linear distance $\sim 2.8 \mu\text{m}$, which was significantly larger than the average ripple size, to enable a correct determination of the peak-difference correlation function.⁶ The inset shows a line fit to estimate the corresponding scaling exponent which was $\alpha = 0.75 \pm 0.04$ ($I_g(r) = I_z(r)^2 \propto r^{2\alpha}$). The lateral correlation length was estimated from the ob-

served knee regime to be $\xi \approx 100$ nm, which is comparable to the ripple size. The oscillatory behavior at larger-length scales ($r > \xi$) can be due to the quasiperiodic structure of the surface topology.⁷

The surface morphology of the Al-Mg alloy [Fig. 1(b)] is close to that of a hill-valley mound structure which is characterized by exponents $\alpha \approx 1$.^{4,7} The knee of the peak-difference correlation function [Fig. 2(b)] suggests a lateral correlation length $\xi \approx 200$ nm, which is approximately half of the observed bump size. The corresponding scaling exponent was estimated to be $\alpha \approx 1.17$. Exponents α close to 1 are characteristic of mound-like structures with a smooth hill-valley morphology.⁴

In conclusion, AES peak profiles can in the weak roughness limit rather closely capture morphology characteristics, enabling possible topological characterization through correlation function measurements. Experimentally, surface roughness effects on Auger peak-line profiles were investigated on specimens with distinct morphologies. The nanometer lateral resolution (~ 15 nm) of the combined scanning Auger/electron microscope system yields peak-line profiles that capture topology variations from flatness down to nanometer-length scales. The peak (-intensity) -difference correlation function $I_z(r)$ at small-length scales revealed a power-law behavior $I_z(r) \propto r^\alpha$, while the corresponding correlation length ξ was comparable to average cluster sizes on the rough surfaces.

The authors would like to acknowledge support from the Netherlands Institute for Metals Research, and the ‘‘Stichting voor Fundamenteel Onderzoek der Materie’’ (FOM-Utrecht), which is financially supported by the Nederlandse Organisatie voor Wetenschappelijk Onderzoek (NOW-The Hague).

APPENDIX

For an element ‘‘a’’ with concentration X_a , the AES electron intensity I_a is given by¹

$$I_a = I_a^0 \int_0^{+\infty} r_a(z) X_a(z) (e^{-z/\lambda_a^0 \cos \phi} / \lambda_a^0 \cos \phi) dz. \quad (\text{A1})$$

For a rough surface with fluctuation amplitude $h(r)$, the lower limit of integration in Eq. (A1) should be replaced by $-h(r)$ and the ϕ by ϕ^* (defined below). Considering the constant element concentration and backscattering factor, we obtain after integration

$$I_a(r) = I_a^0 r_a X_a e^{h(r)/\lambda_a^0 \cos \phi^*}, \quad (\text{A2})$$

$$\cos \phi^* = [\sin \phi (\partial h / \partial r) + \cos \phi] / \sqrt{1 + (\partial h / \partial r)^2},$$

where in the limit of weak roughness, $h(r)/\lambda_a^0 \cos \phi^* < 1$, Eq. (A2) yields $I_a(r) = I_a^0 r_a X_a [1 + h(r)/\lambda_a^0 \cos \phi^*]$. In addition in the limit of the weak local surface slope ($|\partial h / \partial x| \ll 1$), we obtain further for the peak-difference correlation function

$$I_z(r) = \langle [I_a(r) - I_a(0)]^2 \rangle^{1/2} \approx (I_a^0 r_a X_a / \lambda_a^0 \cos \phi) \langle [h(r) - h(0)]^2 \rangle^{1/2}, \quad (\text{A3})$$

with $\langle \dots \rangle$ an ensemble average over possible choices of the origin and roughness configurations, and $\langle [h(r) - h(0)]^2 \rangle^{1/2}$ the height-difference correlation function. The variance of the peak differences, $\langle [I_a(r) - I_a(0)]^2 \rangle$, is denoted by I_g .

¹D. Briggs and M. P. Seah, *Practical Surface Analysis* (Wiley, Chichester, U.K., 1983), Vol. 1.

²M. P. Seah and C. Lea, *Thin Solid Films* **81**, 257 (1981).

³See, for example, see *JAMP 7800 F Scanning Auger and Electron Microscope* (JEOL, Tokyo, Japan).

⁴J. Aué and J. Th. M. De Hosson, *Appl. Phys. Lett.* **71**, 1347 (1997); J. Krim and G. Palasantzas, *Int. J. Mod. Phys. B* **9**, 599 (1995); P. Meakin, *Phys. Rep.* **235**, 1991 (1993); H.-N. Yang, T.-M. Lu, and G.-C. Wang, *Diffraction from Rough Surfaces and Dynamic Growth Fronts* (World Scientific, Singapore, 1993).

⁵See, for example, P. Herrasti, P. Ocon, P. Vazquez, R. C. Salvarezza, J. M. Vara, and A. J. Avria, *Phys. Rev. A* **45**, 7440 (1992); R. C. Salvarezza, P. Vazquez, P. Herrasti, P. Ocon, J. M. Vara, and A. J. Avria, *Europhys. Lett.* **20**, 727 (1992).

⁶G. Palasantzas and J. Krim, *Phys. Rev. Lett.* **73**, 3564 (1994).

⁷Y.-P. Zhao, H.-N. Yang, G.-C. Wang, and T.-M. Lu, *Phys. Rev. B* **57**, 1922 (1998).